NASA TECHNICAL NOTE

NASA TN D-5950

C.1

NASA TN D-5950

TRAJECTORY OBSERVATIONS FOR SOME SPIRALING-ELECTRON BEAM SYSTEMS

by R. W. Wilmarth

Electronics Research Center
Cambridge, Mass. 02139

NATIONAL AERONAUTICS AND SPACE ADMINISTRATION • WASHINGTON, D. C. • MARCH 1971

1. Report No. NASA TN D-5950	2. Government Accession No.	3. Recipient's Catalog No.
4. Title and Subtitle Trajectory Observations for Some Spiraling-Electron Beam Systems		5. Report Date March 1971
		6. Performing Organization Code
7. Author(s) R. W. Wilmarth		8. Performing Organization Report No. C-133
9. Performing Organization Name and Address Electronics Research Center Cambridge, Mass.		10. Work Unit No. 129-02-21-02
		11. Contract or Grant No.
12. Sponsoring Agency Name and Address National Aeronautics and Space Administration		13. Type of Report and Period Covered Technical Note
		14. Sponsoring Agency Code
15. Supplementary Notes		

16. Abstract

A series of experiments dealing with the generation and magnetic compression of periodic electron beams are described. The behavior of these beams was studied using moveable probes and targets as well as photographic techniques. The photographic results are significant in that pictures were obtained under high vacuum conditions such as normally prevail in sealed-off devices. Observations made on partially as well as completely mirrored electron beams are presented.

17. Key Words	18. Distribution Statement
Generation & Magnetic Compression Electron Beams Photographic Techniques	Unclassified - Unlimited

19. Security Classif. (of this report)	20. Security Classif. (of this page)	21. No. of Pages	22. Price*
Unclassified	Unclassified	24	$3.00

*For sale by the National Technical Information Service, Springfield, Virginia 22151

TRAJECTORY OBSERVATIONS FOR SOME SPIRALING-ELECTRON BEAM SYSTEMS

By Robert W. Wilmarth
Electronics Research Center

SUMMARY

A series of experiments dealing with the generation and magnetic compression of periodic electron beams are described. The behavior of these beams was studied using moveable probes and targets as well as photographic techniques. The photographic results are significant in that pictures were obtained under high vacuum conditions such as normally prevail in sealed-off devices. Observations made on partially as well as completely mirrored electron beams are presented.

INTRODUCTION

This paper describes the results of a series of experiments dealing with the generation and magnetic compression of periodic electron beams. These were undertaken as part of the program at this laboratory to investigate electron cyclotron-resonance devices (ref. 1). A number of investigators have designed and built successful devices of this type, (refs. 2, 3, 4); however, to date, no in-depth analytical work has been undertaken to study the behavior of the required electron beams. This is not surprising when one considers the complexities involved with any practical device. For example, a linear electron beam, whether solid or hollow, might first be generated by some standard method. This beam, along with its inherent imperfections, must then undergo a transformation in which the initial longitudinal energy is converted into transverse energy. To properly account analytically for finite beam dimensions, non-uniform magnetic fields and space charge effects is indeed a very difficult problem.

In view of this, a series of experiments were designed to observe the behavior of such beams under various methods and degrees of transformation. In general three methods of observation were employed, namely, photographs of the actual electron beam, obtained by using residual gas ionization; probing with moveable electrodes; and visual observations using moveable targets. The photographic results are probably most significant in that the pictures were obtained under good high vacuum conditions where the effects of positive ions would be minimal.

In fact the photographs were obtained with a vacuum of the degree normally achieved in operating devices and therefore reflects a realistic picture of what is taking place.

In the sections that follow the results of two different methods of electron beam transformation are reported. In Part I, the initial electron beam is generated by a rectilinear-beam gun immersed in a uniform magnetic field. Upon emerging from the gun the beam is passed through a deflection system which imparts some transverse motion to the beam. Because of the magnetic field the beam now follows a helical trajectory about the axis of the system. In Part II the initial electron beam is generated by a hollow rectilinear-beam gun immersed in a uniform magnetic field. Upon emerging from the gun this beam is passed through a region of abrupt magnetic field reversal which imparts a uniform rotation to the beam that is symmetrical to the axis of the system. In both of the above cases, the electron beams were then allowed to drift into regions of gradually increasing magnetic field. The fields were adjusted so that the increase in magnetic field over the axial distance equal to the axial displacement of an electron during one cyclotron period was small. Under these conditions, adiabatic processes prevailed with the result that the magnetic moment was conserved as the beams were both slowed down and compressed. When the system was adjusted for complete conversion of axial energy into transverse energy the magnetic mirror effect was observed. In the experiments described in Part I photographs of actual mirroring were obtained.

PART I - ELECTRON BEAM GENERATED BY A RECTILINEAR-BEAM GUN IMMERSED IN A UNIFORM MAGNETIC FIELD

Experimental Setup

In describing the approach used let us first refer to Figure 1. In order to visually observe the behavior of an electron beam that is immersed in an axial magnetic field, it was necessary to devise a "see-through" magnetic system. This was accomplished by constructing a two layer solenoid with adequate space between adjacent turns and aligning the cross over regions of the inner and outer layers to occur at that side of the coils facing the camera. The solenoid was wound with 0.125 inch diameter copper tubing with a winding pitch of 0.250 inch. This provided a series of 0.125 inch wide viewing regions. The two layer system was used first to reduce the power required and secondly to have any skew effects of the inner layer essentially cancelled by the outer layer. The system was cooled by passing water through the tubing. Figure 2 is a photograph of the complete system which in Figure 3 the bell jar cover has been removed. The actual solenoid which is visible in Figure 3, has an inside diameter of 1.75 inches and is 14 inches long. The coil could be operated continuously at 150 Gauss and intermittently at 200 Gauss. The cathode of the electron gun was placed approximately two coil diameters into the solenoid. From this location to the far end of the field-of-view, a distance of approximately 8 inches, the

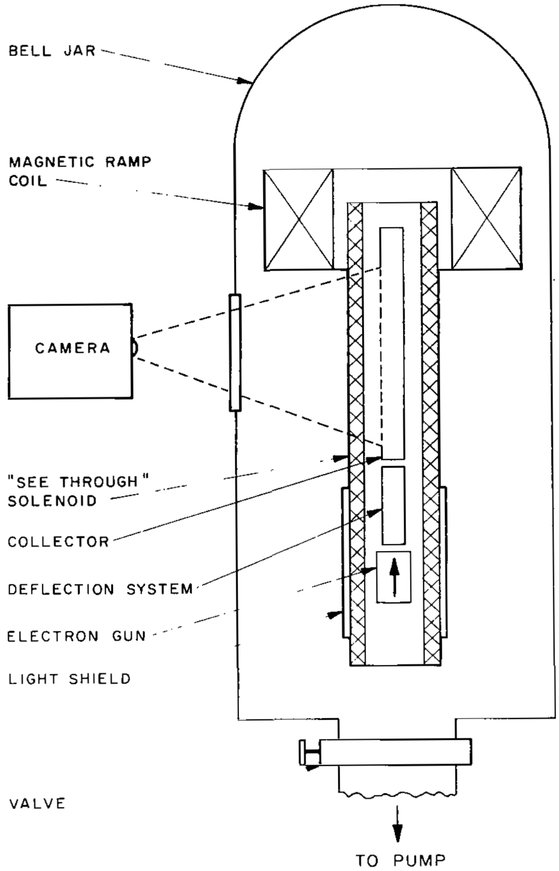

Figure 1.- Part I - Experimental arrangement

axial field was uniform to better than 1 percent, with uniformity across any transverse plane under 0.1 percent. The ramp field was provided by an auxiliary coil as depicted in Figure 1 and visible in Figure 3. This is a multi-layer solenoid encased in a vacuum tight, water-cooled, non-magnetic jacket, designed to operate continuously with a central-point axial field in excess of 500 Gauss. From the figures, it is seen that this coil is located at the collector end of the see-through coil. With both coils operating the net axial field is a superposition of the fields generated by each coil alone. It was found that both coils produced an axial field profile that was essentially flat in the gun region and increased by a factor of approximately three in the viewing region.

Two electron guns were used with this system and both were designed for simple rectilinear flow. The first gun produced a 2-mm diameter beam at a microperveance of 0.236, while the second gun produced a 1-mm diameter beam and a microperveance of

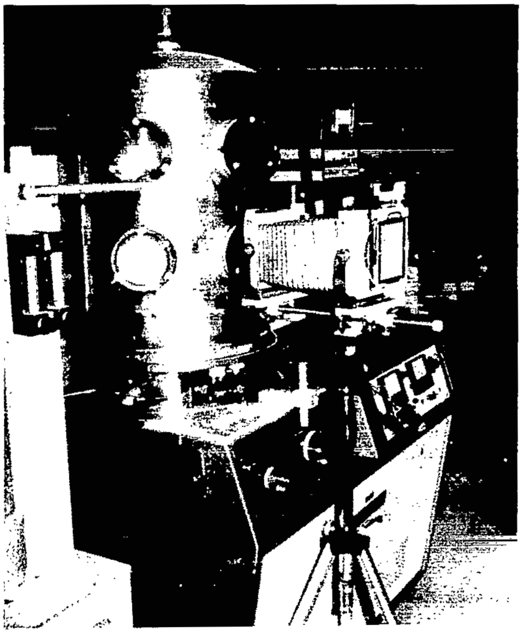

Figure 2.- Experimental system

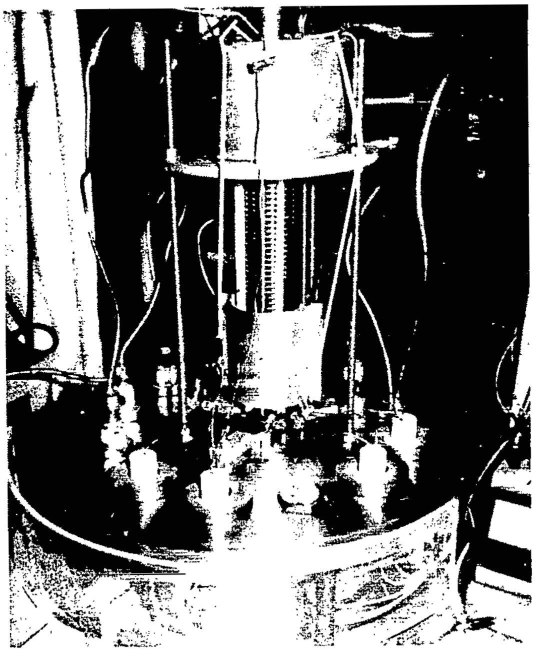

Figure 3.- System with bell jar removed

0.059. Since the perveance and area ratios are related by a factor of four, the beam current density was identical at the same voltage. Both guns utilized tungsten dispenser cathodes which permitted a number of different experiments to be made without disturbing the gun itself.

An interesting part of these experiments was photographing the electron beam. Referring to Figure 1, it is seen that a metal bell jar system is used. Care was taken to block off all unused viewing ports and to provide a light shield between the camera and the jar so as to eliminate any unwanted room light. Within the jar, a light shield was placed around the electron gun to reduce heater-cathode glow from being reflected about the jar. A photograph of a portion of the collector used is shown in Figure 4. It is slotted at the same pitch as the solenoid for viewing and the inside was coated with aquadag to reduce cathode reflections. Any photographic image of the beam is due to ionization of the residual gas in the path of the beam. The brightness of the image obtained depends primarily upon three factors, namely the current in the beam, the system pressure and the length of exposure. All pictures were obtained with ASA 3000 speed film while typical exposures were of four minutes duration at f5.6. With the experiment operating the best vacuum obtainable was 7×10^{-8} Torr. This could be easily and accurately controlled to greater than 1×10^{-6} Torr by adjusting the main gate valve.

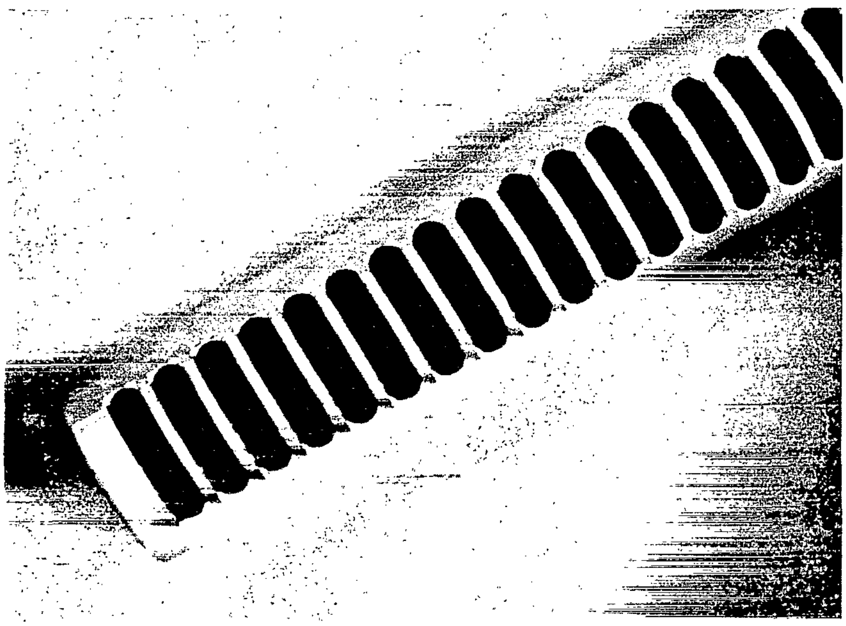

Figure 4.- Slotted collector

A series of pictures were taken at different pressure levels to determine the effects, if any, of positive ions. Most important, there were no discernible changes observed in the beam image as the pressure was adjusted over the aforementioned range. However, two other effects were evident. First, as expected, the lower the pressure the longer the exposure time required. Secondly, a long exposure would tend to result in an overexposure of mechanical components such as the magnet and collector. An optimum pressure was determined to be 8.5×10^{-7} Torr at which good photographs were obtained. The images obtained were identical to those observed at the lower pressure using a much longer exposure. Moreover, the results were always repeatable even when taken weeks apart.

Deflection Schemes

In many of the experiments performed with cyclotron-resonance transverse-wave tubes the initial degree of transverse motion imparted to the electron beam was generated using a magnetic corkscrew (ref. 5). In the experiments described in Part I of this paper, only electro-static deflection schemes were studied. The rationale for studying the electro-static systems was based on the possibility that an electro-static system would be lighter and/or more efficient than a magnetic system.

The first deflection system used could be described as an electro-static corkscrew and consisted of a helical electrode inside a cylindrical electrode. By applying a potential between these electrodes it is evident that transverse electric fields are established which would affect an electron beam moving down the axis of the system. When this system is immersed in an axial magnetic field then the emerging electron beam must follow a helical path. If the transverse energy is gained at the expense of axial energy then the motion within the deflection system is complicated by the fact that the radius of helical trajectory will increase as the pitch of the trajectory decreases. If, however, we require only a small energy conversion to take place within the deflection system then the configuration of the helical electrode is easily determined by assuming pure helical motion. The pitch of the helical electrode is easily found by determining the axial distance an electron travels in one cyclotron period. The axial velocity, ν_{ox}, is related to the beam voltage V_B according to Eq. 1, where $\eta = \frac{e}{m}$.

$$\nu_{ox} = \sqrt{2 \eta V_B} \tag{1}$$

The cyclotron frequency f_c of an orbiting electron is directly related to the magnetic field in gauss as

$$f_c = \frac{\eta B}{2\pi} \tag{2}$$

If we express the velocity as a distance p (pitch) divided by time and the frequency as the reciprocal of time we can simply equate the above expressions and by eliminating the time variable obtain the following relation

$$p = \frac{2\pi}{B}\sqrt{\frac{2V_B}{\eta}} \tag{3}$$

The helical electrode was thus designed using those values of voltage and magnetic field which were convenient to the adjustment range of our equipment. This resulted in a pitch of 1.44 inches. The first deflection system tested utilized a 3-1/2 turn 0.6875 inch diameter helix. In the second series of tests the helical scheme was replaced by a pair of simple deflection plates, while in the last series of experiments a pair of single-turn bifilar helices were used. The merits of each system will be discussed in the following section after the results are presented.

Discussion and Results

When the experiment was first set up a series of initial pictures were taken to first determine the proper exposure conditions, and finally if the corkscrew was working in the prescribed fashion. Proper corkscrew action was verified by first obtaining a spiraling beam and then reversing the direction of the magnetic field. With the field reversed the beam passed through the system with no noticeable effect, even with increased corkscrew deflection voltage. With the field in the proper direction the general validity of Eq. (3) was observed over a wide range of magnetic field and beam voltage. In addition the "resonance" of the corkscrew was evident even with 30 percent of the original beam energy converted to transverse energy. Figures 5 and 6 are typical of the results observed with all three deflection schemes. An interesting observation was that without any deflection voltage the normal scalloping of the straight beam was evident in the photographs even though the envelope variations were small. Unfortunately with an immersed gun it was not possible to set up Brillouin flow. In Figure 7 it is seen that even with a relatively high degree of transverse motion the initial scallops are carried along on the spiraling beam and that each spiral period is very nearly identical with all other periods. At least this was the case over the field-of-view which in some cases covered as many as six periods. However, as the deflection was increased towards the maximum energy conversion (30 percent) the beam outline became fuzzy and progressive periods began to "wash out".

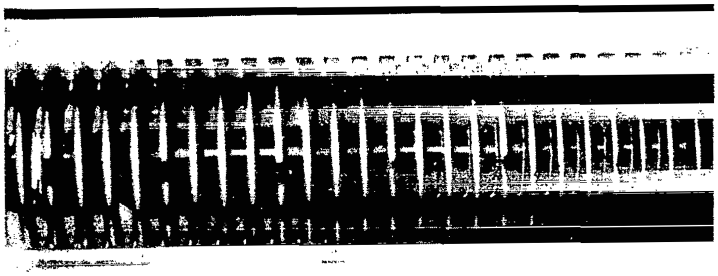

Figure 5.- Photograph of undeflected electron beam

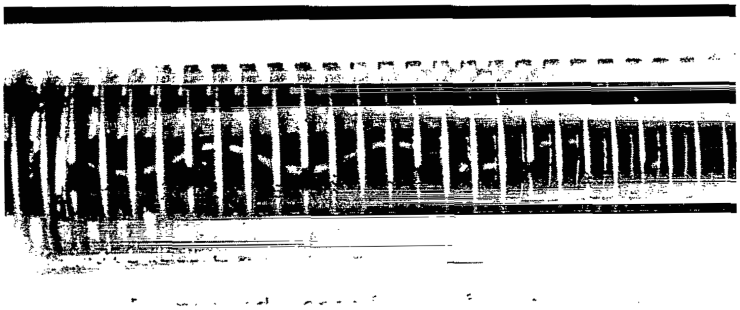

Figure 6.- Spiraling electron beam

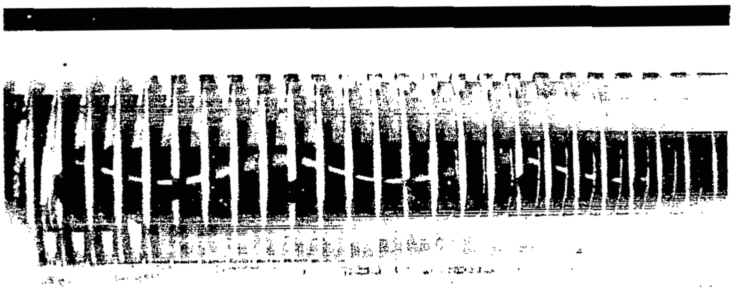

Figure 7.- Spiraling electron beam with scallops

The interesting observation is that the "wash out" appears to be in the axial direction with the radial amplitude remaining essentially constant. This may be a form of axial space charge spreading since electrons may move in an axial direction without crossing magnetic flux lines.

Following the initial experiments with the single-helix deflection scheme, the system was modified by the addition of the ramp coil for further observations of electron beam behavior. Two more deflection schemes; namely, a pair of short deflection plates and a pair of short bifilar helices were studied. In reviewing the results of all three arrangements, including the results obtained with ramp fields present, it is difficult to say which system is the best. However, the simple deflection plates are certainly the least complicated from a mechanical viewpoint and will perform regardless of the direction of the magnetic field. In addition the simple plates are not limited to the conditions of Eq. (3) as in with a corkscrew system. From rf measurements it appears that it is sufficient to convert no more than 10 percent of the axial energy into transverse energy before the magnetic ramp. In the case of Figure 6, 28 percent of the axial energy has been converted into transverse energy. If the conversion were reduced to 10 percent then the ratio of radial displacement to the period in the spiraling beam would be approximately 5 percent. Under these conditions we could not detect any changes within the beam itself over that of the undeflected beam while every periodic variation appeared identical to its neighbors.

Before presenting the results of the ramp experiments let us first consider what might be the expected behavior of a spiraling electron beam injected into an increasing magnetic field. A quantity of interest is the magnetic moment, μ, of an orbiting electron and is defined as

$$\mu = \frac{e^2\Psi}{2\pi m} \tag{4}$$

where e is the charge of the particle, m is the mass and $\Psi=\pi r^2 B$, the flux enclosed by the orbit. It can be shown (ref. 6) that if any magnetic field variations, in either space and/or time, are slow then the moment remains nearly constant and is called an "adiabatic invariant". In terms of the radius of gyration Eq. (4) can be rewritten as

$$\mu = \frac{e^2 r^2 B}{2m} \tag{5}$$

If now the moment is to remain constant as the field is increased from an initial value of B_1 to some value B_2 then the radius of gyration will be decreased as the ratio $(B_1/B_2)^{\frac{1}{2}}$. In addition the transverse component of kinetic energy of the particle would be increased as B_2/B_1.

Now for an orbiting electron drifting into a region of increasing B as would be the case with our electron beam, the axial energy must also be considered. To do this we must require that the total energy of the beam, E, be conserved as expressed in Eq. (6).

$$E = eV_o = \tfrac{1}{2}m\nu_o^{\ 2} + \tfrac{1}{2}m\nu_z^{\ 2} \tag{6}$$

where V_o is the beam voltage, and ν_o and ν_z are the transverse and axial components of velocity. In terms of the magnetic moment the above equation can be rewritten as

$$eV_o = \mu B + \tfrac{1}{2}m\nu_z^{\ 2} \tag{7}$$

and solving for ν_z we get

$$\nu_z = \left[\frac{m}{2}\ (eV_o - \mu B)\right]^{\frac{1}{2}} \tag{8}$$

From the above it is seen that ν_z goes to zero if $eV_o = \mu B$. This is the requirement for the magnetic mirror effect and in terms of initial and final magnetic fields we can write

$$B_2 = \frac{2V_o}{\eta r_1^2 B_1} \tag{9}$$

where $\eta = e/m$. If now B_2 is adjusted to some smaller value than required to satisfy Eq. (9) then the beam would continue along the system in a "tighter" helical trajectory. Figure 8 is a photograph of a spiraling beam progressing down such a magnetic ramp. The reduction in the helical diameter as well as period is evident.

Figure 8.- Electron beam progressing down a magnetic ramp

Figures 9 and 10 show what happens when the ramp field is increased and mirroring begins to take place. In Figure 11 complete mirroring has taken place as the collector current has been reduced to near zero. Further increasing of the ramp field simply increases the slope of the ramp and forces mirroring to take place in a shorter axial distance.

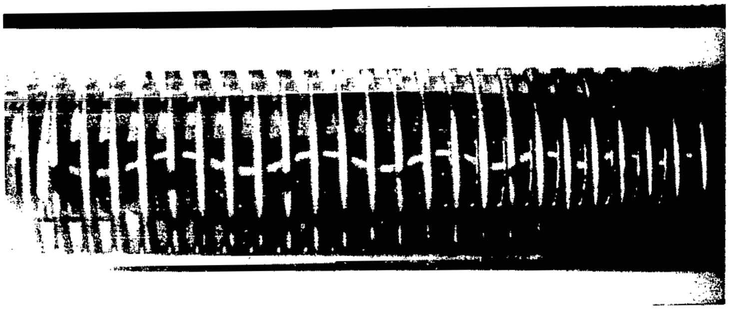

Figure 9.- Onset of mirroring

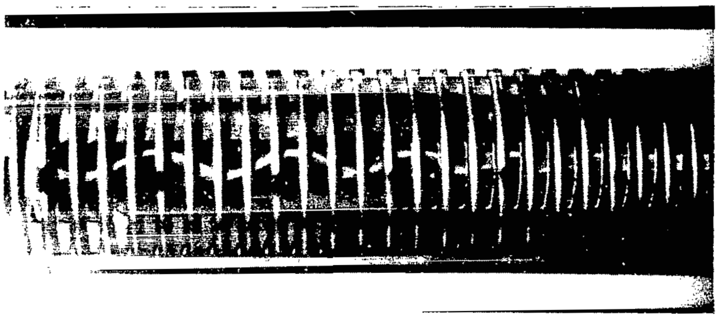

Figure 10.- Partial mirroring

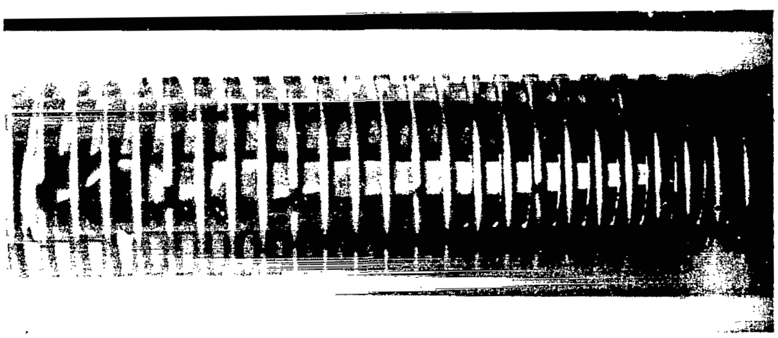

Figure 11.- Completely mirrored electron beam

In studying the photographs two observations were made. First it was noticed that as the ramp field is increased and the beam is compressed, the character of the beam begins to become "washed out" in the mirror region. This is particularly evident in Figure 11 and will be discussed in the following section. Secondly,in some of our photographs, striations were evident on the mirrored beam. The slope of these striations are such that they are not the image of the incoming beam but could perhaps be attributed to some form of circumferential interference taking place between the incoming and mirrored electrons. At present we have no satisfactory explanation for the effect.

In considering the "wash out" of the beam, three effects immediately come to mind. The first would be a velocity spread in the initial beam due to thermal electrons. The second is due to space charge forces, and since electrons must spend a relatively long time in the mirror region this effect would be enhanced. Thirdly, because of the finite dimensions of the beam, electrons in any given transverse plane cannot receive equal treatment from the magnetic ramp. It is most likely that the "washout" is due to a complex combination of these effects. Furthermore, while this paper does not consider it, there is also a possibility that rf growing waves are generated and contribute to the effect.

Further measurements were taken with the system modified to include a moveable collector so that the current distribution as a function of distance could be studied. The moveable collector consisted of a copper rod located within the collector and insulated from it by a boron nitride sleeve. The rod was coupled to a linear motion feed - through seal located in the top port of the bell jar. With this arrangement the rod could be moved through an axial distance in excess of six inches. The electrical connection was made directly through the feed-through seal which was electrically isolated from the bell jar. With the system operating the rod was withdrawn from the field of view and the mirror conditions of Figure 11 were established. The rod was then moved back, step by step, towards the cathode while all parameters were monitored and a photograph of the beam was taken for each step. The results of the photographs were surprising in that as the collector was moved down the beam towards the gun the appearance of the beam up to the collector did not change. It was expected that as those electrons which previously would be mirrored were collected, the fuzziness of the incoming beam would disappear and its spiral character enhanced. Since this was not the case it seems most likely that electrons are mirrored over a considerable axial distance, with the slower electrons being returned first. If we now look at the collector current as a function of position as shown in Figure 12 we see a kind of cyclic variation followed by a decided decline in the region where most of the mirroring took place. It is believed that the cyclic variation is due to secondary emission effects of near mirroring electrons impinging on the flat end of the collector. The fact that the fuzziness was evident with most of the current being collected, as indicated by the plateau region of Figure 12, must mean that the early mirrored electrons spend a relatively long time near one axial location with an increased possibility of initiating ionization.

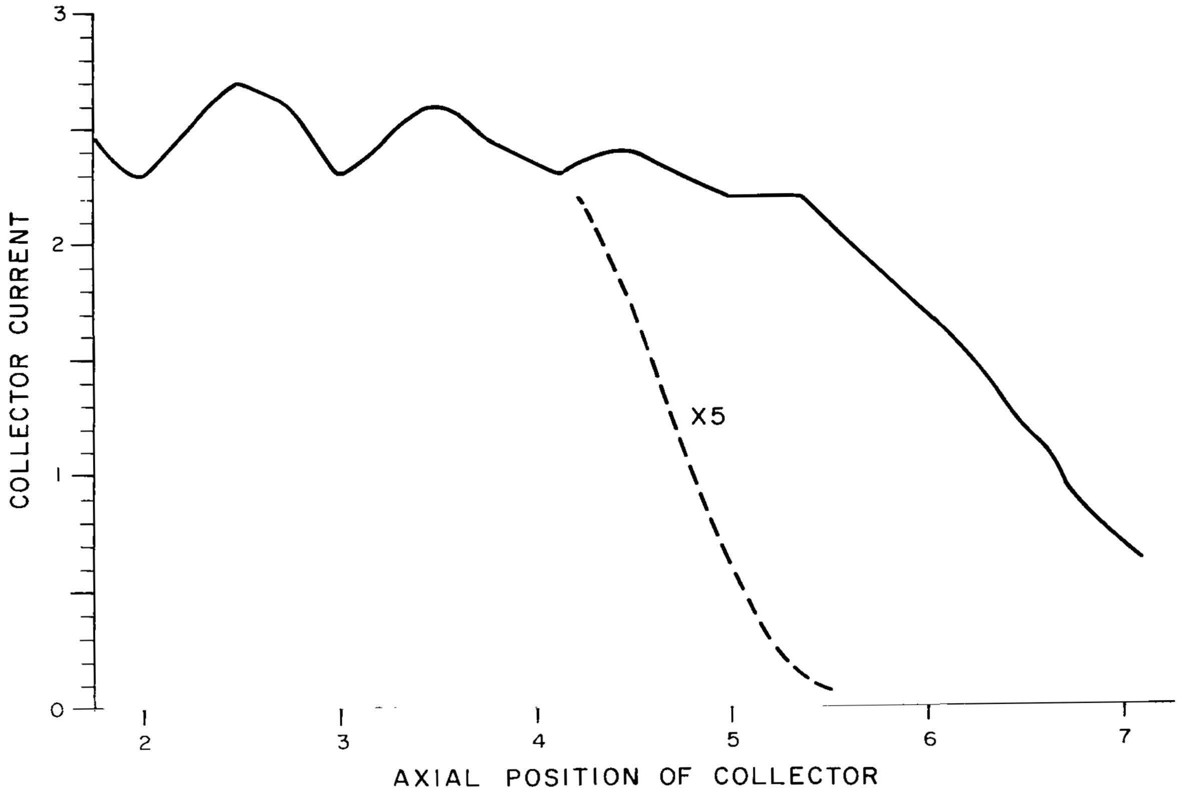

Figure 12.- Collector current as a function of position

In reviewing the results it was believed that the primary cause of the long "wash out" region was due primarily to the thickness of the beam and its unequal treatment in the ramp rather than due to an initial velocity spread. If we consider a simplified magnetic ramp field configuration as shown in Figure 13 then it is evident that in any transverse plane the axial and transverse components are a function of radius. It is also evident that the thicker a beam is, the more unequal the effect will be on electrons occupying the same axial position but at different sides of the beam in the radial direction. While it is true that there is rotation within the beam itself, it is highly unlikely that this would result in an overall improvement in the situation.

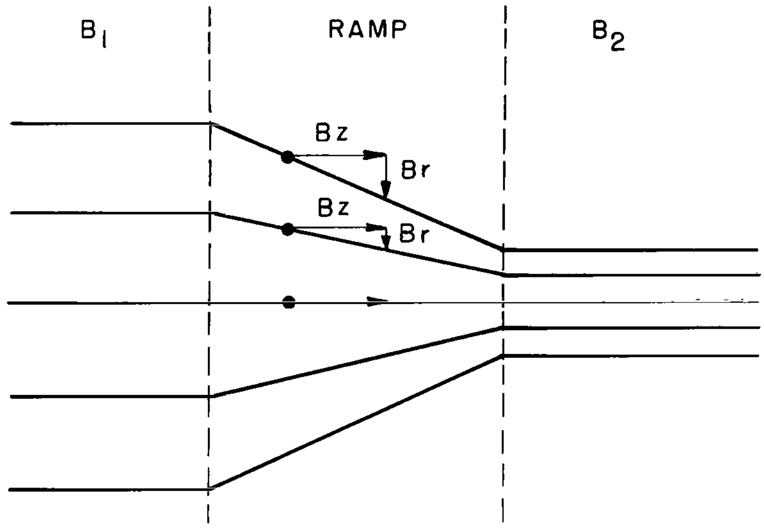

Figure 13.- Simplified magnetic ramp field

In order to strengthen this conclusion a new gun was designed which produced a beam one-half the diameter of the old gun while the perveance was adjusted to maintain the same current density at the same beam voltage. With this gun installed in the system the earlier experiments were repeated. While the beam photographs were lighter due to reduced total current the individual character of the beam persisted for a much greater axial distance while the hazy mirror region was correspondingly shortened. In addition the moveable collector measurements revealed that the current decreased in the mirror region at twice the rate obtained with the larger diameter beam. This is shown in Figure 12 as the dashed line.

PART II - ELECTRON BEAM GENERATED BY A HOLLOW RECTILINEAR-BEAM GUN IMMERSED IN A UNIFORM MAGNETIC FIELD

While it is apparent that a thin or filamentary electron beam is desirable for uniform treatment in a magnetic ramp, it is also evident that a vanishingly thin beam is not practical since current density cannot be increased indefinitely.

Consider now that in any given transverse plane the axially symmetric magnetic ramp varies only in the radial direction. This suggests that we can alleviate the current density problem if we resort to a thin hollow electron beam symmetrically disposed about the axis of the system. For the system to perform however, the electron beam must be rotating. In the experiments described in this section such a beam was generated using an immersed flow hollow-beam electron gun and then passing the beam through an abrupt magnetic field reversal. The behavior of an electron beam in an axially symmetric magnetic field is described by Busch's Theorem as given in Eq. (10).

$$r_1^2\dot{\theta}_1 - r_2^2\dot{\theta} = \frac{\eta}{2\pi}(\psi_1 - \psi_2) \tag{10}$$

In this expression r is the radial coordinate, $\dot{\theta}$ is the angular velocity and ψ is the flux enclosed by the orbit, while the subscripts relate to two different axial positions. The important property described by Busch's Theorem is that the change in angular velocity of an electron between two axial locations depends only on the difference between the total fluxes linked by the orbits and is independent of the trajectory between these two points.

To apply this to the system under consideration let us refer to Figure 14. In region 1 the conditions of an immersed flow rectilinear gun would apply, namely, there would be no angular velocity on the beam, or $\dot{\theta}_1 = 0$. Next it is assumed that the transition region is sufficiently short such that the radius of an electron in traversing the transition remains constant. Finally at the reversal only the direction of the magnetic field is changed while the magnitude remains constant, that is $B_2 = -B_1$. Inserting these conditions in Eq. (10) we find that $\dot{\theta}_2 = \eta B_1$ or in essence the beam is now rotating about the axis at the full cyclotron frequency. Note that this result is independent of radius. In any practical system however, the beam would have finite thickness which means that an electron at the larger radius must have more transverse energy since $v_\theta = r\dot{\theta}$. For total energy to be conserved then the outer electron must have a smaller component of axial velocity. In other words we have a "slipping-stream" hollow beam. Fortunately however this spread can be kept small by making the beam very thin. While space charge effects will be present it has been assumed that these also will be small throughout the reversal region due to the reduced current density in a hollow beam configuration.

Based upon these considerations a hollow beam system was designed and will now be discussed.

Experimental Setup

Figure 15 is a schematic of the system tested while Figure 16 is a photograph of the test setup. In designing the experiment it was decided that the "see through" arrangement used in Part I of this paper was not readily adaptable because of the shielding requirements of the magnetic circuit. It was decided therefore to view the beam using a visible target that would be moveable from near the gun through the peaks of the ramp field. The target consisted of a 0.001 inch thick carbon sheet 0.750 inch in diameter. The movement was controlled via a magnetic coupling

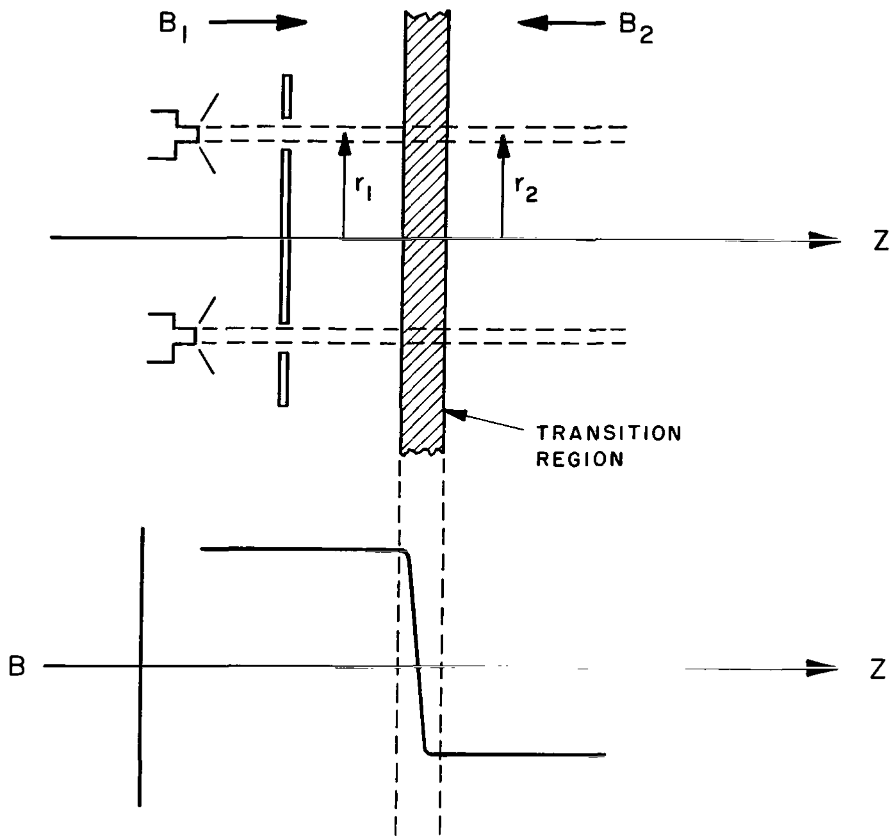

Figure 14.- Field reversal arrangement

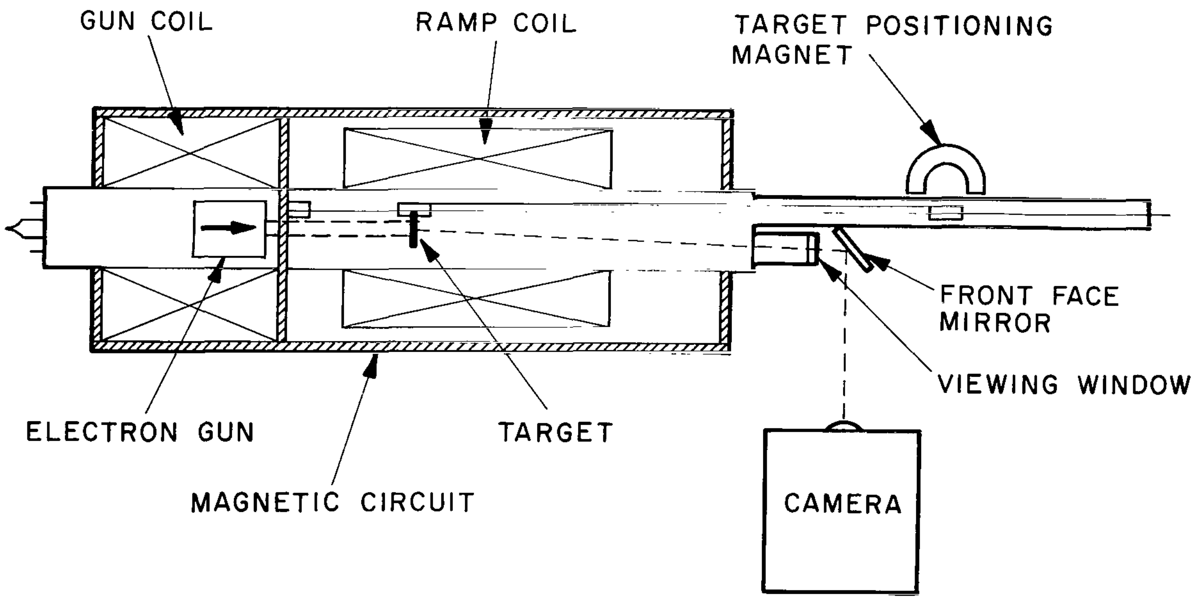

Figure 15.- Part II - Experimental arrangement

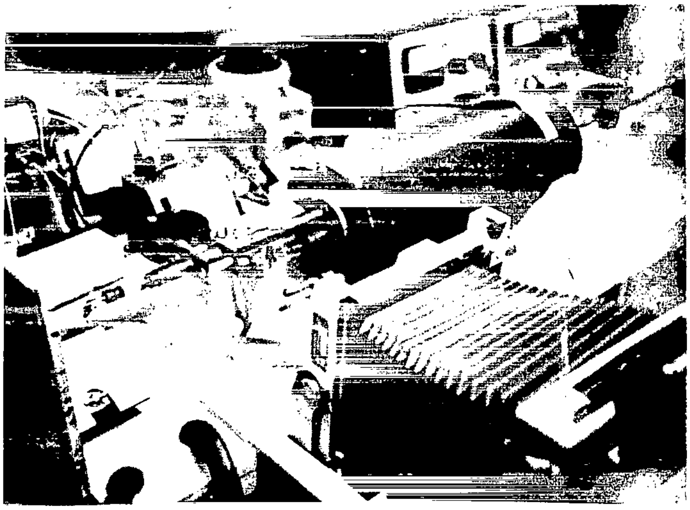

Figure 16.- Part II - Experimental system

located remotely from the beam region. When the experiment was first put into operation, an image was obtained and the camera adjusted for sharp focus. In subsequent observations the target and camera were moved in unison. By back illuminating the target support frame a reference calibration on the size of the image was obtained. The sharpness of the image and the reference calibration were checked over the complete range of the target and found to be consistent. In the experiments the target was moveable over a distance of 5-1/2 inches.

With reference to Figure 15 it is seen that the ramp coil may be positioned over an axial path within the magnetic circuit. This permits some control over the profile of the ramp field as illustrated in Figure 17. Figure 18 is a plot of overall magnetic field profile obtained in the actual experiment. The location of the cathode and the adjustment range of the moveable target are indicated on the plot.

Discussion and Results

When the experiment was first setup and initial images were obtained, a test was performed to see if the experiment was operating to design. With the ramp coil positioned for the minimum degree of ramp profile the field in the gun region was turned off. Inserting the proper initial condition into Eq. 10 (Busch's Theorem) it follows that

$$\dot{\theta}_2 = \frac{\eta B_2}{2} \qquad (11)$$

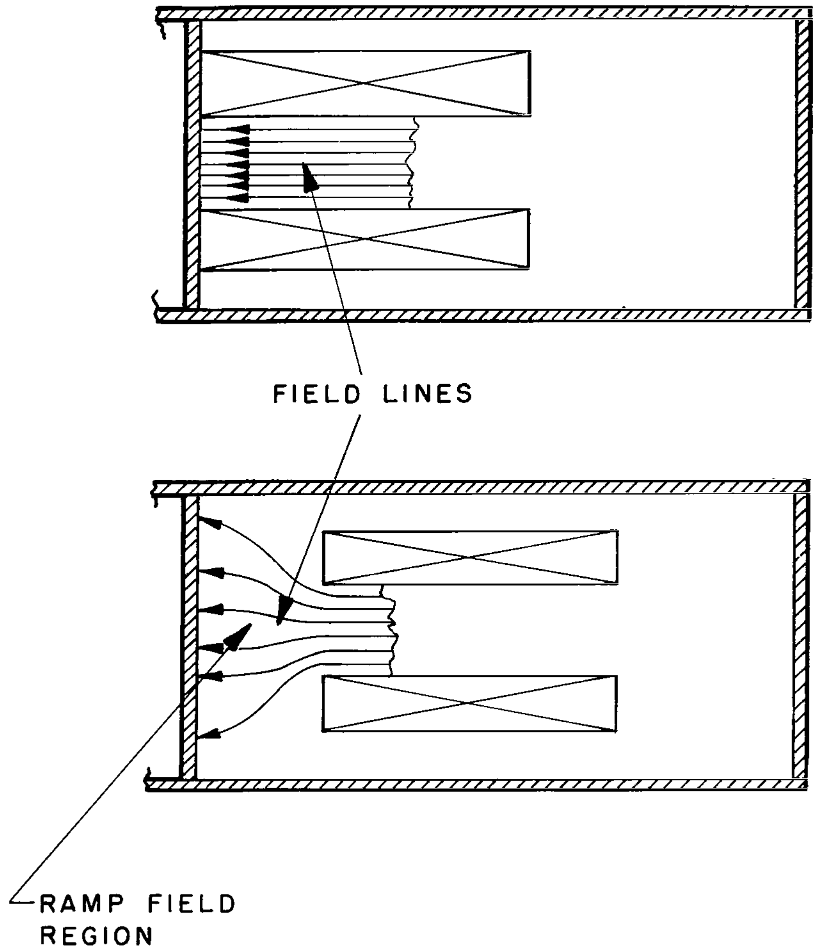

Figure 17.- The effect of positioning the ramp coil

In this expression $\dot{\theta}_2$ is the angular momentum with respect to the axis of the system and is at the Larmor frequency. As far as the electron itself is concerned it is rotating about some other center at the natural cyclotron frequency. The instantaneous velocity of the electron at the point of entry is found by multiplying the angular velocity by the radius and is

$$\nu_\theta = r_2\dot{\theta}_2 = \frac{r_2\eta B_2}{2} \tag{12}$$

Now for an electron orbiting at the cyclotron frequency the radius of the orbit is given as

$$r_c = \frac{\nu_\theta}{\eta B_2} \tag{13}$$

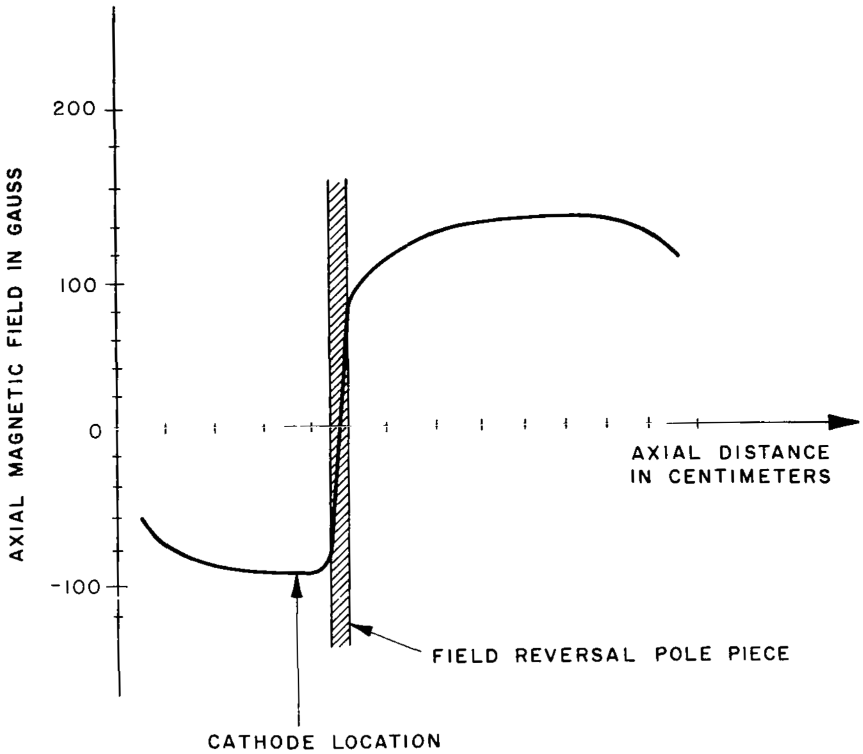

Figure 18.- Magnetic field profile

In our case however, the initial velocities are identical, thus we may combine Eqs. (12) and (13) and obtain

$$r_c = \frac{r_2}{2} \tag{14}$$

This is significant in that it says that the electron must pass through the axis of the system. The situation is illustrated in Figure 19. Now the time required for an electron to make one revolution at the cyclotron frequency is given by

$$t = \frac{2\pi r_c}{\nu_\theta} \tag{15}$$

If we define the distance between successive crossings of the axis as λ_z, we can determine that

$$\lambda_z = \nu_z t = \frac{2\pi}{\eta B_2} \nu_z \tag{16}$$

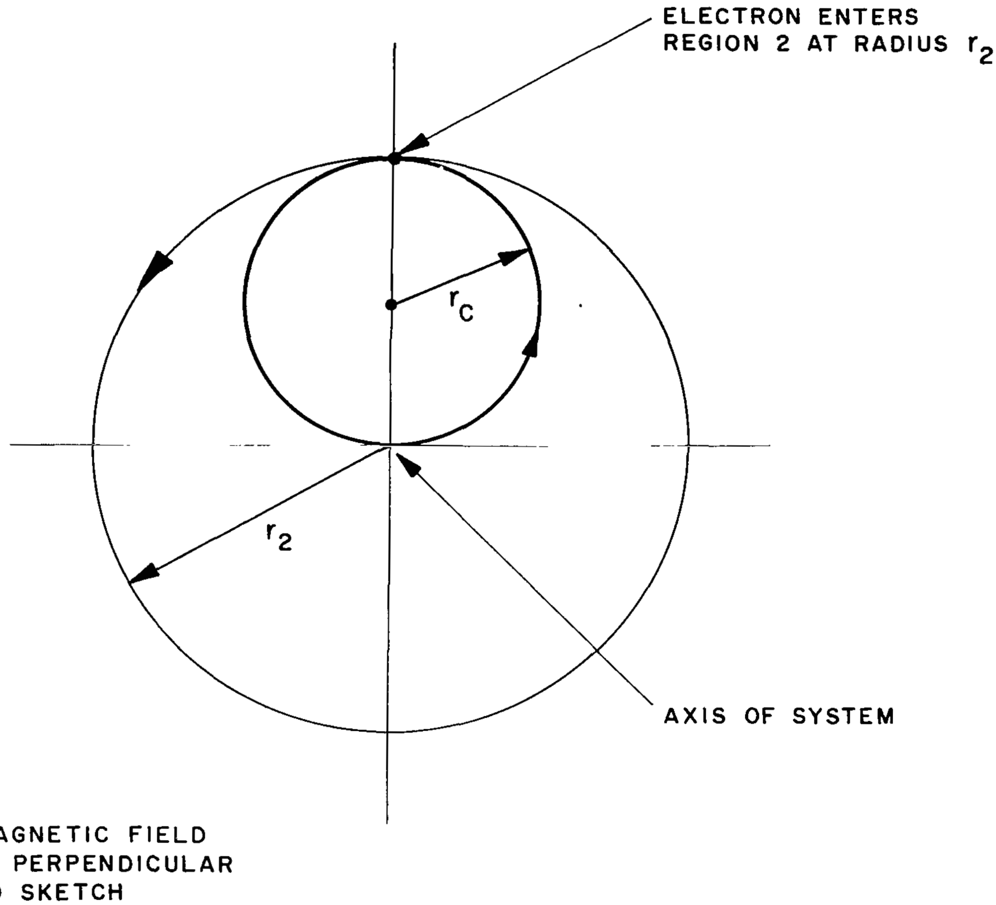

Figure 19.- Electron behavior from axial viewpoint

It should be noted that this result is independent of either r_2 or r_c and involves ν_z. In order to have an explicit expression for λ_z it is necessary to consider the total energy involved as expressed by Eq. (6). By combining Eqs. (16) and (6) to eliminate ν_z we obtain that

$$\lambda_z = \sqrt{\frac{8\pi^2 V_o}{\eta B_2^2} - r_2^2\pi^2} \tag{17}$$

With a completely symmetrical system the beam cross section at any axial position should be perfectly annular except at the point of intersection with the axis where ideally all electrons are focused to a point. The sharpness of these points can be taken as an indication of how well the system is performing. With a ramp field present successive periods of λ_z should be reduced.

In the experimental test with $B_1 = 0$, the beam was focused into a well defined spot while in between axial crossings an annular image was obtained. It was estimated that the spot size was about 0.030 inches in diameter, and represented a power density in excess of 800 watts/cm^2. The axial spacings of the spots were in excellent agreement with Eq. (17). In addition no degradation of spot size could be detected between three crossovers that fell within the movement range of the target.

With the gun field B_1, restored, a clear annular image was obtained throughout the target range. While some scalloping was present on the beam the image was clear and well behaved. At one time in the experiment a visual observation of the spiral character of the beam was made. This was unexpected and occurred because of a small pinhole in the target which permitted a thread of electrons to progress down the tube. The image was faintly visible to the eye only after all room lights were turned off for an extended period and ones eyes became accustomed to the darkened conditions. It should be pointed out that a good vacuum ($<10^{-7}$Torr) was maintained during this observation.

In the ensuing experiments the magnetic fields were adjusted for mirroring and near mirroring conditions while a series of photographs were taken for various positions of the target. Since the target could be accurately positioned and its current monitored the current versus distance profile of the beam was obtained. This result is shown in Figure 20. In comparing this result with those in Part I of this paper it is seen that the fall off in current at the mirror is more abrupt indicating an improvement.

The photographs of the mirrored beam were most interesting in that the results were somewhat unexpected. As shown in Figure 21, a well defined image is obtained up to the position corresponding to the knee of the curve at which place the thickness of the annulus suddenly broadens. This effect, shown in Figure 22, is believed due to the reduction in axial velocity which permits space charge forces to take over. It was found that this effect will also occur if the ramp field is reduced just enough to allow all of the beam to barely pass by. That is, the broadening of the beam annulus did occur in a slowly drifting beam and was evident only after the point of near turn around was traversed.

Before concluding this part of this paper, a few remarks on the properties and effects of the carbon target are in order. First it must be recognized that the resolution of such a target is limited by diffusion of the current-generated heat. In our case however, the target used was extremely thin, and sharply defined images were obtained. Next it should be pointed out that with conditions adjusted for mirroring of the beam, the target

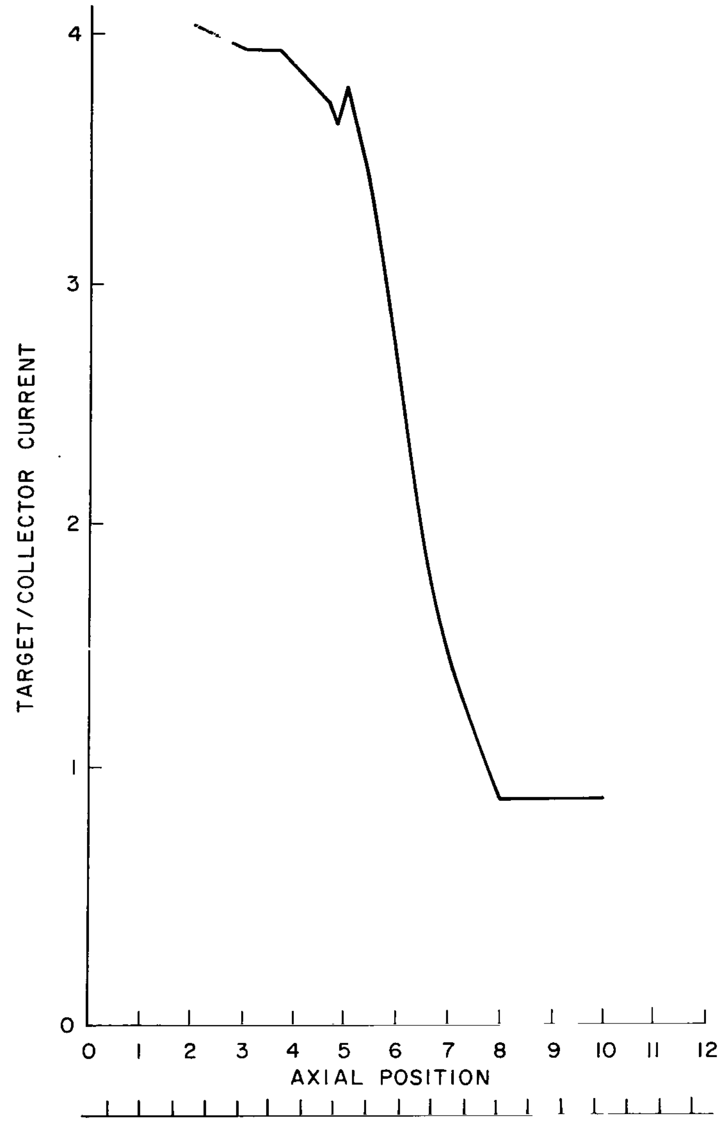

Figure 20.- Collector current as a function of the axial position of the collector

will present an image of only the incoming beam and these are not the same conditions that would obtain in the beam if the target were removed and electrons were allowed to proceed to the mirror and be reflected back through the incoming beam. It is believed however, that our measurements were not greatly affected by the presence of the target. In support of this view, reference is made to the experiments described in Part I of this paper where a mirroring beam was both probed with a moving collector and photographed at the same time. It will be recalled that the presence of the collector did not affect the appearance of the beam.

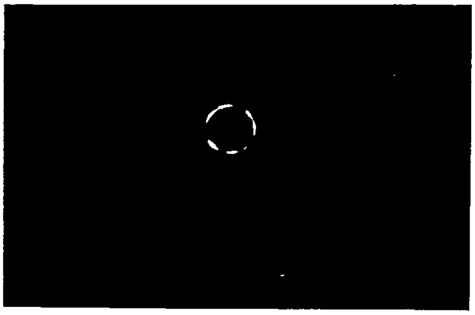

Figure 21.- Rotating annular electron beam

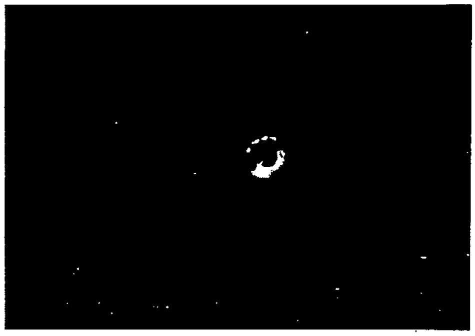

Figure 22.- Annular electron beam at magnetic mirror

CONCLUSIONS

An experimental approach to studying the behavior of an electron beam in a complex environment has been presented. The character of a spiraling beam under near mirroring conditions has been found to "wash out" as space charge forces become important. It has been shown that there are advantages in using a thin hollow electron beam in a magnetic ramp. While a hollow beam electron gun and magnetic field reversal scheme is relatively more complicated than a simple gun and corkscrew deflection system it was shown that such a system is both feasible and well behaved.

REFERENCES

1. Kulke, B.: Design Considerations for Cyclotron Resonance Oscillators. NASA TN-D-5237, June 1969.
2. Hirshfield, J. L.; Bernstein, I. B.; and Watchel, J. M.: Cyclotron Resonance Interaction of Microwaves with Energetic Electrons. IEEE J. Quantum Electronics, Vol. QE-1, September 1965, pp. 237-245.
3. Schriever, R. L.; and Johnson, C. C.: A Rotating Beam Waveguide Oscillator. Proc. IEEE, Vol. 54, 1966, pp. 2029-2030.
4. Kulke, B.; and Wilmarth, R. W.: Small-Signal and Saturation Characteristics of an X-Band Cyclotron-Resonance Maser. Proc. IEEE, (Letters), Vol. 57, February 1969.
5. Wingerson, R.: Corkscrew - A Device for Changing the Magnetic Moment of Charged Particles in a Magnetic Field. Phys. Rev. Letters, Vol. 6, May 1, 1961, pp. 446-448.
6. Spitzer, L. Jr.: Physics of Fully Ionized Gases. Interscience Publishers, Inc., New York, 1956.

NASA-Langley, 1971 —— 25 C-133

NATIONAL AERONAUTICS AND SPACE ADMINISTRATION
WASHINGTON, D. C. 20546

OFFICIAL BUSINESS
PENALTY FOR PRIVATE USE $300

FIRST CLASS MAIL

POSTAGE AND FEES PAID
NATIONAL AERONAUTICS AN
SPACE ADMINISTRATION

09U 001 49 51 3DS 71043 00903
AIR FORCE WEAPONS LABORATORY /WLOL/
KIRTLAND AFB, NEW MEXICO 87117

ATT E. LOU BOWMAN, CHIEF,TECH. LIBRARY

POSTMASTER: If Undeliverable (Section 158 Postal Manual) Do Not Return

"The aeronautical and space activities of the United States shall be conducted so as to contribute . . . to the expansion of human knowledge of phenomena in the atmosphere and space. The Administration shall provide for the widest practicable and appropriate dissemination of information concerning its activities and the results thereof."

—NATIONAL AERONAUTICS AND SPACE ACT OF 1958

NASA SCIENTIFIC AND TECHNICAL PUBLICATIONS

TECHNICAL REPORTS: Scientific and technical information considered important, complete, and a lasting contribution to existing knowledge.

TECHNICAL NOTES: Information less broad in scope but nevertheless of importance as a contribution to existing knowledge.

TECHNICAL MEMORANDUMS: Information receiving limited distribution because of preliminary data, security classification, or other reasons.

CONTRACTOR REPORTS: Scientific and technical information generated under a NASA contract or grant and considered an important contribution to existing knowledge.

TECHNICAL TRANSLATIONS: Information published in a foreign language considered to merit NASA distribution in English.

SPECIAL PUBLICATIONS: Information derived from or of value to NASA activities. Publications include conference proceedings, monographs, data compilations, handbooks, sourcebooks, and special bibliographies.

TECHNOLOGY UTILIZATION PUBLICATIONS: Information on technology used by NASA that may be of particular interest in commercial and other non-aerospace applications. Publications include Tech Briefs, Technology Utilization Reports and Technology Surveys.

Details on the availability of these publications may be obtained from:

SCIENTIFIC AND TECHNICAL INFORMATION OFFICE

NATIONAL AERONAUTICS AND SPACE ADMINISTRATION

Washington, D.C. 20546